

# Prioritize effluent quality, operational costs or global warming? – Using predictive control of wastewater aeration for flexible management of objectives in WRRFs

**Stentoft, Peter Alexander; Munk-Nielsen, T.; Møller, Jan Kloppenborg; Madsen, Henrik; Valverde-Pérez, Borja; Mikkelsen, Peter Steen; Vezzaro, Luca**

*Published in:*
Water Research

*Link to article, DOI:*
10.1016/j.watres.2021.116960

*Publication date:*
2021

*Document Version*
Peer reviewed version

# Prioritize Effluent Quality, Operational Costs or Global Warming? – Using Predictive Control of Wastewater Aeration for Flexible Management of Objectives in WRRFs

**P. A. Stentoft*,**, T. Munk-Nielsen*, J. K. Møller**, H. Madsen**, B. Valverde-Pérez***, P. S. Mikkelsen ***, L. Vezzaro *,*****

* Krüger A/S, Veolia Water Technologies, Denmark (pas@kruger.dk, thm@kruger.dk, lxv@kruger.dk)

** Department of Applied Mathematics and Computer Science, Technical University of Denmark, Denmark (past@dtu.dk, jkmo@dtu.dk, hmad@dtu.dk)

*** Department of Environmental Engineering, Technical University of Denmark, Denmark. (luve@env.dtu.dk, psmi@env.dtu.dk, bvape@env.dtu.dk)

**Abstract:**

This study presents a general model predictive control (MPC) algorithm for optimizing wastewater aeration in Water Resource Recovery Facilities (WRRF) under different management objectives. The flexibility of the MPC is demonstrated by controlling a WRRF under four management objectives, aiming at minimizing: (A) effluent concentrations, (B) electricity consumption, (C) total operations costs (sum electricity costs and discharge effluent tax) or (D) global warming potential (direct and indirect nitrous oxide emissions, and indirect from electricity production) . The MPC is tested with data from the alternating WRRF in Nørre Snede (Denmark) and from the Danish electricity grid. Results showed how the four control objectives resulted in important differences in aeration patterns and in the concentration dynamics over a day. Controls B and C showed similarities when looking at total costs, while similarities in global warming potential for controls A and D suggest that improving effluent quality also reduced greenhouse gases emissions. The MPC flexibility in handling different objectives is shown by using a combined objective function, optimizing both cost and greenhouse emissions. This shows the trade-off between the two objectives, enabling the calculation of marginal costs and thus allowing WRRF operators to carefully evaluate prioritization of management objectives. The long-term MPC performance is evaluated over 51 days covering seasonal and inter-weekly variations. On a daily

basis, control A was 9-30% cheaper on average compared to controls A, D and to the current rule-based control. Similarly, control D resulted on average in 35-43% lower greenhouse gasses daily emission compared to the other controls. Difference between control performance increased for days with greater inter-diurnal variations in electricity price or greenhouse emissions from electricity production, i.e. when MPC has greater possibilities for exploiting input variations. The flexibility of the proposed MPC can easily accommodate for additional control objectives, allowing WRRF operators to quickly adapt the plant operation to new management objectives and to face new performance requirements.

**Keywords**: Activated Sludge, N2O emissions, Nonlinear MPC, Economic MPC

## 1. Introduction

Automatic control strategies have been applied in Water Resource Recovery Facilities (WRRFs) for decades, mainly focusing on improving effluent quality, responding to variations in the inlet pollutant loads, and reducing chemical consumption and energy demand (Yuan et al., 2019). The latter control objective has recently gained increasing attention, as water supply and sanitation uses 2-3% of the world's electrical energy, with ranges around 1-18% in specific urban areas (Olsson, 2015). Specifically, WRRFs are not negligible, using approximately 1% of a country's total electricity consumption (Cao, 2011). This also implies a noticeable carbon footprint for urban water cycles: for example, this is estimated to be 372 kg-$CO_2$/person/year in California, corresponding to 4% of total per capita emissions (Escriva-Bou et al. 2018).

The diffusion of *smart grids*, favoured by the diffusion of solar and wind electricity sources, have triggered several studies which investigated the possibility of moving

WRRF peak consumption in time, thereby decreasing their carbon footprint. Lisk and Long (2013) and Kirchem et al. (2018) concluded that both wastewater transport and treatment can provide substantial flexibility in electricity consumption. Further investigations of the WRRF electricity consumption have identified aeration as the most demanding step, accounting for about 50% of total consumption (Longo et al. 2016). Aeration control is thus essential for the plant economy, carbon footprint and for reducing peak electricity consumption.

Maximizing efficiency in aeration control is a task involving a trade-off of different objectives which might vary over time. Several studies have defined aeration efficiency in terms of energy usage, i.e. to minimize electricity consumption while satisfying effluent limits (Longo et al., 2020, Yuan et al., 2019). This definition assumes that lower electricity consumption would linearly lead to reductions in operational costs and/or in greenhouse gas (GHG) emissions related to the electricity production. Other studies considered effluent quality/cost by introducing weights on concentrations and electricity consumption (Yamanaka et al. 2006). However, the current development in electricity supply, going towards a higher penetration of renewable energy sources (Ren21, 2020), undermines this assumption of a direct correlation between electricity consumption and costs/emissions.

Using Denmark as example, the hourly electricity prices varied between -112.18 DKK/MWh and 385.59 DKK/MWh on the 2019/01/14 (Nordpool, 2020), while the related GHG emissions varied between 42 kg-$CO_2$-eq/MWh and 162 kg-$CO_2$-eq/MWh (Energinet, 2020). This example shows how a minimal electricity consumption does not necessarily lead to minimal operational costs, since a low and constant electricity consumption would not exploit the negative price. If peak prices and emissions are distributed differently over the day, reducing GHG emissions

related to electricity is also different from reducing operational costs or electricity consumption.

An additional operational cost in Denmark is represented by the effluent tax, aiming at reducing N emissions from WRRFs, and set to 30 DKK/kg-N (Danish Ministry of Taxation, 2020). Minimizing aeration can therefore reduce N removal and thereby lead to an increase in total costs. Furthermore, controls varying oxygen conditions may promote direct GHG emissions as $N_2O$, especially at low DO levels (Domingo Félez and Smets, 2019). This can considerably affect the carbon footprint of municipal WRRFs (Delre et al., 2019).

WRRF operators need flexible control strategies capable of operating at the highest level of the control hierarchy, i.e. they should be able to quickly accommodate for different management objectives (effluent quality, operational costs, electricity consumption, GHG-emissions). Model Predictive Control (MPC) fulfils these demands thanks to the possibility of using objective functions considering multiple targets. MPC uses a model of the controlled system to evaluate the effect of different control actions based on an *ad-hoc* objective function, choosing the one ensuring the best outcome. For computational reasons, MPC typically employs simple models. An advantage of MPC is that the control becomes a direct optimization problem where the design of the objective function decides the effective control. Hence, changing the objective function leads to new optima and thereby new control actions. This becomes particularly advantageous when objectives have variable inputs (see e.g. Lund et al. 2018).

Several examples of MPC for WRRF aeration exists in literature, such as MPC based on process models (e.g. Holenda et al., 2008, Mulas et al., 2015), or black-box models using neural networks which learn from data (e.g. Foscolliano et al. 2016, Bernardelli

et al. 2020). However, these examples do not consider varying electricity prices or GHG emissions, and therefore they will not adapt to *smart grid* systems, characterized by price variations or by varying tariffs (as in the example from Aymerich et al. 2015).

Varying prices can be known in advance due to the market mechanics, as in the case of the Nordpool market covering Northern Europe. If variable tariffs are present as in Spain (Aymerich et al. 2015) a price model of the tariffs can supply price variations ahead in time. If prices are uncertain but follow a certain pattern (e.g. diurnal) this can also be incorporated using a price model. Furthermore, GHG-emissions from electricity production can be forecasted using different techniques such as machine-learning (Leerbeck et al. 2020a), creating new opportunities for MPC, which can consider these future variations in the control evaluation. This approach has been tested for integrated control of pumping from sewer system basins to WRRFs (Stentoft et al. 2020a). To the knowledge of the authors, two strategies for predictive control of aeration using electricity price data are found in literature (Stentoft et al. 2019a, Brok et al. 2019). However, these approaches face challenges with long optimization times (Stentoft et al. 2019a) or no direct handling of effluent limits (Brok et al. 2019). Varying GHG emissions in electricity mix have been investigated in the control of heat pumps for district heating systems (Leerbeck et al. 2020b), but not for WRRF aeration. In addition, the trade-off between operation costs and GHG-emissions will become increasingly important in case a $CO_2$ tax is introduced. However, to the authors knowledge this has not been investigated for WRRFs aeration control.

This paper presents a general MPC setup using stochastic differential equations which allows WRRF operators to balance between different management of objectives

without developing a new control strategy, i.e. by simply switching the objective function to optimize e.g. effluent, electricity consumption, aeration costs, and/or GHG emissions. The setup is tested on a small alternating WRRF (i.e. a plant where intermittent aeration allows nitrification and denitrification to occur in the same tank - Isaacs and Thornberg, 1998) in Denmark (Nørre Snede). Four objectives (minimization of effluent N levels, electricity consumption, operational costs, GHG emissions) are tested. The MPC is evaluated by analysing the changes in the aeration set-points defined by the control and the impacts on the plant daily performance and over long term. Furthermore, a combined objective function is assessed, showing how an operator can quickly modify plant operations according to different management of objectives.

## 2. Materials and Methods

### 2.1 Data-driven Activated Sludge Model for nitrogen removal

There are several data-driven models simulating nitrogen removal processes based on stochastic differential equations, including those developed in the 1990s (Carstensen et al. 1995) and recent developments (Stentoft et al. 2019b). Here, an adapted version of Stentoft et al. (2019b) is used. This new version introduces the state $S_\mu$ which models the concentration of ammonium in wastewater arriving at the biological treatment step. In addition the model introduces the algebraic equation, $O$, which describes the alternating aeration signal (eq. 5). The model is derived from the ASM1s process description and it is described by the following set of equations:

$$dS_{NH} = \kappa_1\left(S_\mu + f\ \ (t) - S_{NH}\right)dt - r_{Ni}\frac{O_1(t)S_{NH}}{r_{Ni}K_{NH} + S_{NH} + m_{NH}}dt + \sigma_1 d\omega_1 \quad (1)$$

$$dS_{NO} = \kappa_1\left(\mu_{in,NO} - S_{NH}\right)dt + r_{Ni}\frac{O_2(t)S_{NH}}{r_{Ni}K_{NH} + S_{NH} + m_{NH}}dt - \frac{r_{Dni}\left(1 - O_2(t)\right)S_{NO}}{r_{Dni}K_{NO} + S_{NO} + m_{NO}}dt + \sigma_2 d\omega_2 \quad (2)$$

$$dS_\mu = \kappa_2\left(\mu_{in,NH} - S_\mu\right)dt + \ \sigma_3 d\omega_3 \quad (3)$$

where parameters and state variables are listed in Table 1.

<Table 1>

The term *f(t)* provides an estimate of the diurnal variation in the incoming ammonium load at the biological treatment, inspired by the harmonic formulation suggested by Langergraber et al. (2008).

$$f\ \ (t) = \Sigma_{i=1}^{2} cc_{2i-1}\sin\left(\frac{i\pi t}{p}\right) + cc_{2i}\cos\left(\frac{i\pi t}{p}\right) \quad (4)$$

where *t* is the input time [minutes], *p* is the period of the harmonic functions (1440 minutes for a diurnal variation), and the parameters $cc_x$ define the shape of the harmonic profiles.

The terms $O_1(t)$ and $O_2(t)$ in eq. 1-2 represent a formulation of the alternating aeration signal with different delay for ammonium and nitrate. Here the aeration is modelled as a sum of sigmoid-functions which allows for direct estimation of the delay $D_1$, $D_2$ in the system. This should here be seen as a late response from when aeration starts/stops ($\tau_{on}/\tau_{off}$) to the moment when there are observable changes in ammonium/nitrate concentrations, as also described in Stentoft et al. (2017):

$$O_j\left(t, \tau_{on}, \tau_{off}\right) = \sum_{i=0}^{n} \frac{1}{(1+e^{\alpha_1})^{\kappa_3}(1+e^{\alpha_2})^{-\kappa_3}} \quad (5a)$$

$$\alpha_1 = -\kappa_4(t - \tau_{on,i} - D_j) \quad (5b)$$

$$\alpha_2 = t - \tau_{off,i} - D_j \quad (5c)$$

In an online setting, the switching times, $\tau_{on}/\tau_{off}$, are determined from the control DO set-points simply by defining $\tau_{on}$ as the times when the DO set-point switches from zero to a value greater than zero and vice versa (for $\tau_{off}$). All the additional parameters (listed in Table 1) are estimated automatically, without the need for manual interventions, by minimizing a negative log likelihood function using a gradient-based optimizer with respect to the last 24 hours of data. The setup is more thoroughly described in Stentoft et al. (2019b). The modelling framework specified here (and in Stentoft et al. 2019b) is designed to run online with parameters being re-estimated frequently (i.e. every 6-12 hours). This implies that changes in the biological processes or incoming water are captured when the parameters in the model

are updated. If changes are expected more frequently, the parameter update frequency can be increased. The uncertainty of the model (i.e. the variance/covariance matrix) is estimated using the Extended Kalman Filter (EKF) to update the model states with observations and a numerical integration scheme. This is thoroughly described in Stentoft et al. 2019.

## 2.2 Nonlinear Model Predictive Control of Activated Sludge Processes

Model Predictive Control (MPC) finds the best control action(s) based on an optimization over future objectives with respect to some objective function, $J(u)$ with inputs $u$, and $m$ constraints $b_i$ on a constraint function $l(u)$. Typically this is set up as a minimization problem, and it can generally be expressed as

$$min\, J(u) \tag{6a}$$

$$s.t.\, l_i(u) \leq b_i, i = 1, \dots, m \tag{6b}$$

If either the objective function, $J(u)$, or the constraint function, $l_i(u)$, is a nonlinear function, the problem becomes a nonlinear optimization problem. This is more difficult to handle compared to a linear or convex optimization, and thereby it allows for fewer optimization variables. However, it has the major advantage that it can embrace non-linear system dynamics. The challenge in nonlinear optimization is that the objective can have several local optima, requiring good initial parameter guesses or optimization algorithms that can efficiently explore the parameter space (Lund et al. 2018). This is further elaborated for this application in Section 2.4.

In this MPC implementation, the goal is to find the best aeration strategy that minimizes different objectives with respect to constraints on the process and on the aeration signal itself. The aeration signal is here optimized with respect to when it

should be switched "on"/"off" as the DO-setpoint is set simply as a function of ammonium concentration. Hence constraints on the aeration signal can be expressed using simple linear constraints that govern how long aeration equipment can be "on" and "off":

$$\tau_{on,i} - \tau_{off,i} \leq \tau_{max,on} \quad (7a)$$

$$\tau_{on,i} - \tau_{off,i} \geq \tau_{min,on} \quad (7b)$$

$$\tau_{off,i} - \tau_{on,i+1} \leq \tau_{max,off} \quad (7c)$$

$$\tau_{off,i} - \tau_{on,i+1} \geq \tau_{min,off} \quad (7d)$$

Where the difference, $\tau_{on,i} - \tau_{off,i}$, represents the time interval when aeration is active ("on"), and $\tau_{off,i} - \tau_{on,i+1}$ the period when aeration is off. These time differences have also a lower ($\tau_{min,on}$, $\tau_{min,off}$) and an upper ($\tau_{max,on}$, $\tau_{max,off}$) constraint, which are set by experienced process engineers to avoid detrimental effect on the biological communities in the plant.

Biological tanks are assumed to be completely mixed reactors, i.e. effluent concentration limits for ammonium ($L_{NH}$) and total nitrogen ($L_N$) can be added as constraints:

$$E_{24h}[S_{NH}] \leq L_{NH} \quad (8a)$$

$$E_{24h}[S_{NO} + S_{NH}] \leq L_N \quad (8b)$$

where $E_{24h}[S_x]$ are the 24-hour average effluent concentrations, which according to the Danish legislation need to comply with effluent discharge limits. Additional constrains can be added to comply with local discharge regulations, targeting e.g. instantaneous discharge limits.

## 2.3 Flexible control of management objectives

To investigate the response of a WRRF controlled by the presented MPC, four different management objectives are investigated:

- *Objective A: Effluent total-N optimization*, considering only the mean effluent concentration of ammonium and nitrate.
- *Objective B: Electricity consumption optimization*, considering only aeration on-time;
- *Objective C: Total operational costs optimization*, considering electricity consumption and effluent taxes;
- *Objective D: Global Warming Potential (GWP) optimization*, considering $N_2O$ direct emissions from nitrogen removal and indirect from N discharged in the effluent, as well as indirect greenhouse gas emissions (GHG) related to electricity production;

The *optimization of effluent total-N* (A) minimizes the sum of ammonium and nitrate in the effluent over the 24-hour prediction horizon, in line with the Danish discharge regulation.

$$J_{(A)}(\tau_{on}, \tau_{off}) = \int_{t=0}^{24h} (S_{NH}(t) + S_{NO}(t))\, dt \tag{9}$$

The *optimization of electricity consumption* (B) assumes that aeration is the most energy-intensive step in a WRRF and does not consider variations in electricity prices. This scenario minimizes the objective function $J_B$, which estimates the total time aeration is activated during the 24-hour prediction horizon:

$$J_{(B)}(\tau_{on}, \tau_{off}) = \int_{t=0}^{24h} Air_{on}(\tau_{on}, \tau_{off}, t)\, dt \tag{10}$$

where the term $Air_{on}(\tau_{on}, \tau_{off}, t)$ [-] is an indicator function tracking the aeration status (set to 1 if aeration is on at time t and 0 otherwise).

The *optimization of total operational costs* (C) further extends objectives (A) and (B) for areas with varying electricity prices or a tax on effluent nutrients. This scenario minimizes the objective function $J_C$ similar to the one used by Stentoft et al. (2019a), which expresses the total cost in Danish Krone (DKK). This considers both the effluent discharge tax on total-N ($T_N$ [DKK/gN]) and the hourly electricity price (from the day-ahead market) at the *t-th* hour ($Ep_t$ [DKK/MW]) multiplied with the constant *Ec* [MW] which is the electricity consumption of the aeration equipment.:

$$J_{(C)}(\tau_{on}, \tau_{off}) = \int_{t=0}^{24h} \left(Ep_t Air_{on}(\tau_{on}, \tau_{off}, t) Ec + (S_{NH}(t) + S_{NO}(t)) T_N\right)\, dt \tag{11}$$

*The optimization of global warming potential* (D) minimizes the objective function $J_D$ which consider the total GHG emissions as $CO_2$ equivalent [kg-$CO_2$-eq]:

$$J_{(D)}(\tau_{on},\tau_{off}) = \int_{t=0}^{24h} \Big( R_{N_2O}\left(r_{NH}(t,\tau_{on},\tau_{off})\right) C_{N_2O,CO_2} + (S_{NH}(t) + S_{NO}(t)) Eff_{N_2O} C_{N_2O,CO_2} + GHG_{El,k} Air_{on}(\tau_{on},\tau_{off},t) \Big)\, dt \quad (12)$$

where the term $R_{N_2O}$ is the effective rate at which $N_2O$ is created as a function of the ammonium removal rate $r_{NH}$. This can be estimated as the term from (1):

$$r_{NH} = r_{Ni} \frac{O_1(t,\theta) S_{NH}}{r_{Ni} K_{NH} + S_{NH} + m_{NH}} dt \quad (13)$$

This objective function thus considers $N_2O$ production as a function of ammonia removal rate, modelled according to two correlations found in Blum et al. (2018). This model considers $N_2O$ emissions by nitrifying nitrification pathway, which is dominant in several plant configurations working with ammonia based aeration control when nitrification capacity is limited (e.g., winter time; Ahn et al., 2010, Porro et al., 2017, Bellandi et al., 2020). In addition, indirect $N_2O$ emissions due to nitrogen discharged in the effluent are estimated as a fraction of effluent total nitrogen ($Eff_{N2O}$) that is calculated based on IPCC guidelines (Bartram et al., 2019). Indirect GHG emissions from electricity production in the Danish market ($GHG_{El,k}$) are calculated based on data from Danish electricity network operator, presented in section 2.5 (Energinet, 2020).

To illustrate how the MPC can combine different management objectives, a combined objective function $J_{(C,D)}(\tau_{on},\tau_{off})$ is used, where a weight α [-] is used to prioritize among the different objectives:

$$J_{(C,D)}(\tau_{on}, \tau_{off}) = \alpha J_{(D)}(\tau_{on}, \tau_{off}) + (1-\alpha) J_{(C)}(\tau_{on}, \tau_{off}) \quad (14)$$

Where α ranges between 0, giving full priority to costs minimization, and 1, giving full priority to minimizing GHG emissions.

**2.4 Simplifications for implementation in an online setup**

All the considered objective functions are non-linear. Since the number of switching times (i.e. the controlled variables which govern when aeration is switched on and off) increase with the length of horizon, the optimization can become difficult for long horizons (i.e. the period ahead in time which the MPC strategy optimizes). Hence, simplifications are needed to speed up the calculation time and to reduce the number of parameters to be estimated, thereby enabling the application of the proposed MPC in an online setup.

Here a prediction horizon of 24 hours is considered as the legislation requirements consider 24 hour average effluent concentrations. The calculations of the constrains on the 24 hour effluent concentrations (eq. 8a,b) are implemented by adding two state variables to those listed in eq. 1-3: average ammonium, $S_{\mu,24h,NH}$, and average total-N, $S_{\mu,24h,N}$.

$$S_{\mu,24h,NH} = \frac{\int_{t=0}^{24h} S_{NH} dt}{24h} \quad (15a)$$

$$S_{\mu,24h,N} = S_{\mu,24h,NH} + \frac{\int_{t=0}^{24h} S_{NO} dt}{24h} \quad (15b)$$

These new states can be seen as mean concentration over time as the integral sums the concentrations over the 24 hr horizon.

In case of very low discharge limits or extraordinarily high incoming nutrient loads, the MPC might fail to satisfy the constraints on the effluent 24h average concentration (eq. 8a,b). Nevertheless, the optimizer should still be capable of providing an acceptable solution with respect to eq. 8, disregarding the objective function *J*. From a MPC point of view, this implies that eq. 8 should be implemented as soft constraints i.e., as an expression added directly in the objective function. Hence two additional terms are added to the functions $J_{A\text{-}D}$.

$$P_{NH} = \frac{ze^{S_{\mu,24h,NH}}}{1 + e^{-100(S_{\mu,24h,NH} - L_{NH})}} \tag{16a}$$

$$P_N = \frac{ze^{S_{\mu,24h,N}}}{1 + e^{-100(S_{\mu,24h,N} - L_N)}} \tag{16b}$$

Where the constant z is a sufficiently large number which secures that the penalties $P_{NH}$ and $P_N$ are prioritized over other terms in the objective function when the means $S_{\mu,24h,NH}$ and $S_{\mu,24h,N}$ are larger than the limits $L_{NH}$ and $L_N$ respectively.

The number of parameters to optimize is reduced by parameterizing the vectors of switching times, $\tau_{on}$ /$\tau_{off}$. Here the parameterization of $\tau_{on,i}$ /$\tau_{off,i}$ also includes the constraints on the aeration equipment (eq. 7) and new input vectors, $k_{on}$ /$k_{off}$ which consist of real numbers (and fewer control variables as compared to optimizing directly on the switching times, $\tau_{on}$ /$\tau_{off}$).

$$\tau_{on,i}\left(k_{on}, \tau_{max,on}, \tau_{min,on}, \tau_{on,i-1}\right) = \tau_{on,i-1} + \tau_{min,on} + \frac{\tau_{max,on} - \tau_{min,on}}{1 + e^{Sp(k_{on})}} \quad (17a)$$

$$\tau_{off,i}\left(k_{off}, \tau_{max,off}, \tau_{min,off}, \tau_{off,i-1}\right) = \tau_{off,i-1} + \tau_{min,off} + \frac{\tau_{max,off} - \tau_{min,off}}{1 + e^{Sp(k_{off})}} \quad (17b)$$

326

327 The function $sp(..)$ is a periodic spline function with coefficients described by the
328 input vectors $k_{on}$ and $k_{off}$. This implementation allows choosing how many splines
329 and thus how many parameters, $k_{on}$, $k_{off}$, are needed for the optimization.
330 Generally, a greater number of parameters allows for a more detailed optimization of
331 the controlled process, but results in a greater number of local minima, thus becoming
332 more difficult to optimize. Here a total of 12 parameters are found to be sufficient
333 considering the dynamics and inputs.

334

335 The relatively low number of optimization variables, combined with the fast
336 evaluation of the objective function, allows for the use of global optimization
337 algorithms to minimize the objective function. In this study, the Shuffled Complex
338 Evolution (SCE) algorithm (Duan et al., 1993) is used. SCE is run with a maximum of
339 5000 function evaluations, taking approximately 60 seconds to run on a normal PC
340 (CPU is an Intel Core i7-6600 with 2.60 GHz), and, generally, ensuring convergence
341 to the global optimum. This is considered sufficient, as decisions should, not be made
342 more often than every 20 minutes. The model and optimization algorithm are
343 implemented in R and $C^{++}$, using the TMB package for R (Kristensen et al. 2016).

This package compiles the model written in $C^{++}$ and supplies the objective function as an R-object for easy use with various optimization algorithms.

### 2.5 Case study

The presented MPC setup is tested by using data from the Nørre Snede WRRF (Denmark). This is a small plant with a biological treatment volume of 3500$m^3$ and an average daily inlet volume of 1.350$m^3$ (in dry weather), yielding a hydraulic retention time of 2.6 days. The biological reactor is bottom aerated. Air diffusers are operated with alternating control, which implies that water is aerated in cycles to shift between aerobic and anoxic conditions (referred to as "on" and "off" control or intermittent aeration). Intermittent aeration at Nørre Snede WRRF is currently controlled using an advanced Rule-Based Control (RBC) strategy, which switches aeration on and off as a function of online ammonium and nitrate measurements taken every 5 minutes (Isaacs and Thornberg, 1998). Additionally, DO set-point is controlled as a function of the latest ammonia measurement every 2 minutes, following a cascade control structure (larger ammonia concentrations results in higher DO set-points – cf. Isaacs and Thornberg, 1998). The main scope for this control is simultaneous carbon and nutrient removal, as phosphorus is removed using chemical precipitation. However, carbon is not monitored at Nørre Snede WRRF, as WRRF designed for nitrogen removal demand large SRTs which sustain effective carbon removal. The plant is further described in Stentoft et al. (2019b).

Volatile suspended solids are assumed to be 3g-VSS/L, typical for activated sludge systems (Tchobanoglous et al. 2004). The different constants related to the objectives listed in section 2.3 are summarized for Nørre Snede WRRF in Table 1.

<Table 2>

Hourly electricity prices ($Ep_t$) for the Denmark West market were retrieved from the public online databases of the European power exchange Nord Pool (Nordpool, 2020). Similarly, 5-minute GHG emissions from electricity production ($GHG_{El,k}$) were retrieved from public databases of the Danish electricity grid operator (Energinet, 2020).

Figure 1 shows daily prices and GHG emissions for 51 days in the period from 2019/01/14 to 2020/02/18, highlighting both inter- and intra-daily variations. The first day (2019/01/14) is chosen as an example to illustrate the MPC response to daily variation. The subsequent 51 days are chosen at an 8-day interval in order to obtain a dataset that is equally distributed among different weekdays and covers all year seasons.

<Figure 1>

**2.6 MPC Evaluation**

The performance and verification of the presented MPC is investigated by looking at different aspects using the MPC model described in section 2.1 and the specifications of constraints and control in section 2.2-2.4.

*WRRF daily performance under different management objectives*

To qualitatively verify the MPC implementation and to compare the effects on the WRRF performance of the four management objectives listed in section 2.3, a first analysis is performed on aggregated daily values, followed by a comparison of the plant outlet over the 24-hr period covering the example day (2019/01/14). The plant performance is evaluated using different performance indicators, reflecting the different management objectives, and compared against the existing control (RBC):

- Effluent quality, expressed by $NH_4$, $NO_3$ and total-N effluent concentrations, to evaluate performance in nutrient removal;
- Operational costs, calculated as total costs, electricity costs and effluent taxation costs, to evaluate financial performance;
- Efficiency indicators, expressed by relative aeration on-time, average electricity consumption and average electricity GWP emissions. This is to evaluate the control prioritizes with respect to the inputs
- GWP indicators, expressed as total GHG emissions, $N_2O$-emissions and indirect GHG emissions, from electricity consumption, to evaluate climate performance.

The MPC evaluation uses the model parameters listed in Table 1, and the electricity prices and GHG emissions highlighted in Figure 1.

The MPC response to dynamics in electricity costs and GHG emissions is investigated by looking at the cumulative functions of total costs and GHG emissions over the optimization horizon.

*MPC response to varying effluent limits*

To verify the correct implementation of soft constrains and to evaluate the MPC response to different discharge limits, 30 different optimizations are run for each

management objective by increasing the limit $L_{NH}$ in steps of 0.05 from 0.5 to 2 mgN/L.

*Multiple objectives and marginal costs*

To verify eq. 14, The function and trade-off are evaluated by using a sequence of values for $\alpha$, ranging from 0 to 1. Furthermore, this objective function makes it possible to investigate the marginal costs of preferring GWP compared to total costs.

*Long term performance evaluation*

The proposed MPC is used to control WRRF operation over the 51 days shown in Figure 1: given four different objectives, this yields to 204 optimizations in total. Potential correlations between intra-diurnal differences in costs, $id_{cost}$, and GHG emissions, $id_{GHG}$, in the optimized objective function values are investigated using these 204 optimizations.

$$id_{cost} = J_{(B)} - J_{(C)} \tag{18a}$$

$$id_{GWP} = J_{(A)} - J_{(D)} \tag{18b}$$

## 3. RESULTS AND DISCUSSION

### 3.1 Model implementation

The estimated model parameters from Nørre Snede WRRF for the example day are listed in Table 1 with a description. An example of model fit with a 3 hour prediction is shown in Figure 2.

<Figure 2>

Figure 2 shows how the model captures the dynamics of the alternating control as the concentrations increase/decrease as expected when aeration is turned on/off. In addition, the uncertainty of the model seems reasonable as it increases with the prediction horizon, which during the estimation period is only until next available observation. This model is used in the following as basis for the predictive control.

### 3.2 WRRF daily performance under different management objectives

Figure 3 shows the optimal control obtained in the four management objectives for the example day (Figure 1).

<Figure 3>
<Table 3>

The dynamics seen in Figure 3 and the WRRF performance indicators for the whole day (Table 3) highlight some interesting findings.

*Effluent quality*

The differences in the concentration values and dynamics under the different optimization objectives are clearly shown. All objectives comply with the soft constraints in (eq. 16). The greatest difference is noted when using function $J_{(C)}$ (Figure 3a), which has longer aeration phases and short non-aerated intervals in the

early morning and minimizes aeration in the afternoon. This is a direct response to the negative electricity prices between 00:00 and 05:00 (Figure 1a), which are exploited by the MPC. The effluent concentrations under objective A and D show similar patterns, but ammonium concentrations are slightly higher in objective D, meaning that less aeration is used. This is the consequence of the minimization of carbon footprint derived from energy used for aeration. The ammonium concentrations are generally increased for objective B, where electricity is minimized. Here ammonium is kept as high as possible within constraints (1.5 mg-N/l).

*Operational costs*

The average price of consumed electricity (i.e. the price when electricity is used) is approximately 30% lower for objective C compared to the others (Table 3; 174.2 vs 247.5, 245.7, 248.0 and 259.8 DKK/MWh), while smaller differences are observed among the other objectives. The electricity cost for RBC is slightly higher, due to a long non-aerated phase during the negative price period. The lowest electricity cost is (C), even though it uses more electricity compared to both (B) and the RBC. The difference in electricity costs of (A), (B), (D) and the RBC are characterized by their differences in relative amount of aeration.

The low average electricity price is also the reason why objective C leads to 13.9% lower total costs (Table 3; 247.7 DKK vs 279.4 DKK), even though it requires 6.2% more aeration compared to objective B (39.5%  vs 33.3% aeration time). It should also be noted that optimizing costs and electricity consumption are, respectively, 19.5% and 9.2% cheaper than the current RBC (which uses 324.2 DKK). This is because of a combination of lower electricity prices (for C), and a better balance

between taxes and electricity consumption achieved by approaching to discharge limits (for B and C).

*GWP*

The average GWP from electricity consumption for (D) is similar to the other strategies indicating that this factor does not necessarily affect the optimal control actions (Table 3; 112.6, 114.0, 102.7, 113.1 and 115.6 kg-CO2-eq/MWh for A-D and RBC respectively) . However, $N_2O$ emissions are 3-4 times larger in , B, C and the RBC compared to A and D (Table 3; 69.2, 282.4, 227.9, 64.7 and 219.6 kg-CO2-eq for A-D and RBC respectively). This corresponds to a reduction in GWP of 50.3%, 42.8% and 42.4% lower in Objective D compared to B, C and the RBC, respectively. This indicates that optimizing for low effluent nitrogen concentration is closer to minimizing GHG emissions and hence plants operated with this management objective might already have lower GWP than plants focusing on other objectives.

Comparing Objective C against B results in a 13.1% lower GWP, suggesting that Objective C, despite higher electricity consumption, is better in terms of both costs and GWP compared to minimization of electricity consumption. This difference is explained by the difference in $N_2O$ emissions, which is investigated further in the next section. Finally, it should be noted that Objective D, optimizing GWP, costs 30.9 % more compared to Objective C, indicating that a trade-off between operational costs and GWP needs to be made by WRRF operators. This picture may change if a $CO_2$ tax on WRRF GHG-emissions is imposed.

**3.3 Objective function dynamics**

513 Figure 4 shows the dynamics of the different strategies in terms of cumulated
514 electricity costs and $N_2O$ emissions over the simulated example day.
515
516 <Figure 4>
517
518 Figure 4 illustrates how the MPC in C exploits better the negative prices, as after the
519 first 8 hours the cumulative cost is still negative. Furthermore the slope on the
520 cumulative curve is less steep compared those of Objectives A and D, resulting in an
521 overall cost reduction. Because of the heavy aeration in the first 10 hours (where
522 electricity prices where low), Objective C also manages to keep ammonium
523 concentrations and therefore it keeps removal rates, sufficiently low to avoid large
524 $N_2O$ emissions during this period. However, Objective D manages to achieve low
525 $N_2O$ emission over the entire horizon by balancing ammonium concentration at a
526 sufficiently low level which keeps the ammonium removal rates (eq. 13) low.
527
528 **3.4 MPC response to varying effluent limits**
529 The total costs and global warming potential that is found when optimizing the same
530 scenario as in Figure 3 is investigated. Here the effluent ammonium limits is changed,
531 and the result is shown in Figure 5.
532
533 <Figure 5>
534
535 At low effluent requirements (i.e. ammonium <0.8 mgN/L) MPC perform similarly
536 for all objectives. This is because the main MPC goal becomes to satisfy effluent limit
537 in all cases. When the effluent limit is increased, it becomes possible for the MPC to

prioritize aeration in different periods and hence different outcomes between objectives are observed. This verifies the effect of the soft-constraint, which dominates the MPC decisions when discharge requirements are not satisfied.

The total operational costs are reduced in all cases until A and D stabilize around 1.25 mg-N/L. This suggests that the effluent requirements are not important for A and D, which already tend to minimize effluent nitrogen emissions. In the case of B and C, total costs are further reduced, and it is likely that for C the cost would decrease further, albeit little, if the limit was increased more than 2 mg-N/L. Surprisingly, the cost of Objective B starts to increase at some point, and thereby the difference between Objective C and B increases above approximately 1.5 mg-N/L. This is because the contribution of the effluent tax to the total costs overcomes the additional savings in electricity consumption.

For GWP, Objective A and D stabilize above 1.25 mg-N/L, suggesting that, as for total costs, effluent requirements become unimportant for MPC. Objective B and C increase GWP until roughly 1.4 mg-N/L, after which they decrease slowly. The initial increase is caused by the higher $N_2O$-emissions as consequence of the lower aeration, which results in higher ammonium removal rates (aeration time is reduced, and thus ammonia oxidation rates increase due to ammonia accumulation). The later decrease in GWP is caused by the fact that the frequency and duration of aeration is so low that the effective aeration time and thus total emissions are reduced, even though the emission rate is high during aeration.

This highlights that with the management objectives from B or C, lower discharge limits do not necessarily lead to better performance in terms of GWP. Furthermore it highlights that indirect $N_2O$ emissions related to total-N in the effluent are comparably much lower than direct emissions from the WRRF.

563

564 **3.5 Multiple objectives and Marginal Costs**

565 Figure 6 compares the operational costs and GWP for the optimization performed by
566 using the combined objective function (eq. 18), showing the trade-off between the two
567 management objectives.

568

569 <Figure 6>

570

571 For example, a reduction of GWP by 125 kg-CO2-eq (42%) results in an increase in
572 costs of about 50 DKK (20%), corresponding to a marginal cost of 0.4 DKK/kg-CO2-
573 eq. This is obtained with a weight α around 0.65 (i.e. MPC puts a 65% weight on
574 GWP and 35% on costs). Figure 6 shows how the trade-off does not follow a linear
575 trend, highlighting how optimization of GWP and total costs require different control
576 actions. Therefore, the marginal cost depends on the chosen weight, and the definition
577 of α thus requires a careful analysis. For instance, high prioritization of GWP ($\alpha$ >0.8)
578 does not lead to important reduction of GWP, but it increases costs from roughly 300
579 to 335 DKK. Arguably WRRF managers should define a weight that balances GHG
580 emission (especially $N_2O$ emission rates) while still leaving the MPC flexibility to
581 exploit the opportunities offered by low electricity prices. In addition, it is noted that
582 $\alpha$ values ranging from 0.2 to 0.75 will lead to a control strategy which in this case
583 performs better than the current RBC on both total costs and GWP.

584

585 **3.6 Long term performance**

586 Figure 7 shows a summary of the results for the four optimization objectives
587 performed over the 51 days shown in Figure 1 in terms of operational costs and GWP
588 indicators.
589
590 <Figure 7>
591 <Figure 8>
592
593 Clearly, better performance is obtained for indicators specifically targeted by the
594 optimization objective. Objective B and C, focusing on reduction of operational costs
595 and electricity, show average costs that are not significantly different (using a 95%
596 confidence level), with only a 3.4% difference (it is though noted that the difference is
597 significantly larger than zero). However, when looking at single days (Figure 8a),
598 differences appear between the two objectives for days with high inter-diurnal
599 variations, while the difference is relatively small for most of the simulated days. It is
600 difficult to conclude whether the relationship is linear or exponential, but it can be
601 observed that the variance also increases with increasing inter-diurnal variations. This
602 trend is interesting when considering that future electricity prices might show even
603 greater inter-diurnal variations due to increasing amounts of renewables (REN21,
604 2020) and/or implementation of varying $CO_2$-dependent taxes/tariffs.
605 Compared to the other objectives, optimizing total costs is significantly cheaper
606 compared to A, D and the baseline RBC, with 29.6%, 19.2% and 9.2% lower costs,
607 respectively. Surprisingly, Objective A, C and D obtain the three lowest minimum
608 costs (leaving out B), as indicated by the bottom of the whiskers in Figure 7(a). These
609 values are all found in a day with 12 hours of negative prices (2019/12/16) when A

610 and D, which prioritize to higher aeration, “earns” money during half of the day while
611 still reducing the effluent tax.
612
613 The GWP is reduced when directly targeted by the objective function (Objective D)
614 or when minimizing N in the effluent (Objective A). D has a mean GWP 42.5%,
615 40.9% and 34.9% lower than B, C and RBC, respectively. When compared to
616 Objective A, the mean is not significantly lower (13.9%) due to the relatively large
617 variances (but, the difference is significantly larger than zero). As for total costs,
618 significant differences between Objective A and D appear when looking at individual
619 days (Figure 8b), with greater divergences in days with greater inter-diurnal variations
620 in GHG emissions from electricity production. However, the trend has a larger
621 variance compared to the one observed for costs, due to the contribution of $N_2O$
622 emissions, which are independent from the electricity source. In both cases, part of the
623 variation can also be explained by the fact that the distribution of highs and lows
624 within the electricity- price/GHG series are important for the actual potential for
625 exploitation. Hence some days are simply easier to distribute aeration in “smart” ways
626 than others.
627 The minimum GWP obtained in Objective C is relatively lower compared to those
628 obtained for B and RBC. This is because the low price periods which are exploited by
629 A have the added benefit that ammonium removal rates become smaller, hence less
630 $N_2O$ is created (as also observed for the example day in Figure 4b). Furthermore, low
631 price periods typically correspond to lower indirect GHG emissions, thanks to the
632 Danish electricity mix. The high extreme value obtained for Objective A (the whisker
633 in Figure 7b) is caused by a day with very high electricity GHG-emissions
634 (2019/05/21, ranging from 259 – 439 kg-CO2-eq/MWh).

635

636 **3.7 Future Outlook**

637 The proposed management objectives can be expanded to enhance the plant
638 performance both in terms of total operational costs and GWP. For example, total
639 costs can be further reduced by including other electricity markets in the objective
640 function. While in this study only the "day-ahead market" is considered, the balancing
641 market (demand-response) seems to be particularly interesting for wastewater
642 treatment (Brok et al., 2019). This expansion would require a stochastic MPC strategy
643 where both upregulation (use less electricity on a short notice) and downregulation
644 (use more electricity on a short notice) are built into the objective function. Variable
645 tariffs which are present in some areas in order to promote peak shaping should also
646 be investigated (Aymerich et al. 2015). Thus, it is noted that the generality of the cost
647 function allows for adding this when creating the future price input. The Danish
648 legislation also taxes phosphorus and organic carbon emissions, creating the
649 possibility for further extension of the objective function. Including these substances
650 would require an additional model using stochastic differential equations (Lindstrøm
651 et al., 2019) which, ideally, should also include predictive control of chemical dosing.
652 Currently the DO setpoint when aeration is "on" is not considered in the MPC.
653 Instead it is set by the plant (in this case as a function of ammonia concentrations).
654 However, to refine the strategy, the specific DO setpoints (and not just the switching
655 times) would be beneficial to include directly in the optimization.

656

657 The calculation of $N_2O$ is based on empirical findings on laboratory scale partial
658 nitritation Anammox reactor, where emissions were driven by nitrifying nitrification
659 pathway (Blum et al., 2018a). We note, however, that heterotrophic and nitrifying

denitrification pathways may also contribute to the overall emissions (Chen et al., 2019) and should be considered for more reliable optimization. There is relatively extensive literature on different statistical models relating different operational parameters and nitrous oxide emissions, which could be applied for the objective function (Vasilaki et al., 2018, Bellandi et al., 2020). Furthermore, these correlations could be re-calibrated with soluble $N_2O$ online data (where available). Additionally, several studies have suggested different ratios and more detailed models, accounting for all pathways contributing to $N_2O$ emissions from activated sludge processes (Domingo Félez and Smets, 2016). This shows how the prediction of $N_2O$ emissions is affected by a large level of uncertainty, which can be overcome by including $N_2O$ as a state in the system of coupled stochastic differential equations. This new state should ideally be calibrated with online $N_2O$ measurements to accommodate changes in plant due to seasonality (i.e., temperature), solid retention time, dissolved oxygen, pH or other crucial parameters (Blum et al., 2018b; Daelman et al., 2015; Massara et al., 2017; Noda et al., 2004). In addition, objective functions that also consider the hydraulic capacity of plants, including secondary clarifiers and return sludge, could be designed. This would be particularly useful for handling increased inlet flow during wet-weather events.

Finally, it is necessary to further validate the MPC framework, as the simple model used for optimizing and evaluating control performance does not include all the biological processes relevant in a WRRF. Further studies are thus suggested for (i) evaluating the MPC using detailed biological models (Henze et al., 2000) both for the tested configuration (alternating plant) and in benchmark setup (Jeppsson et al., 2007); and (ii) full scale testing of the long-term performance of the proposed control strategy.

## 4. Conclusion

A flexible model predictive control (MPC) framework for optimizing aeration in WRRF was presented, allowing WRRF operators to optimize plant controls according to different management objectives over a 24 hour prediction horizon. The framework was tested with data from the Danish electricity grid and the Nørre Snede WRRF. Four different objective functions were investigated and evaluated with an objective analysis using different data inputs. The four objectives minimize total operational costs, electricity consumption, global warming potential (GWP), and effluent total-N.

The study revealed how the four controls resulted in quite different in terms of the resulting aeration patterns, and hence dynamics of ammonium/nitrate concentrations in the biology tanks and in the effluent.

Controls optimizing total costs and electricity consumption both prioritized to aerate less. Controls focusing on effluent quality and GWP both resulted in lower effluent concentrations, showing how a management objective optimizing effluent quality can also be optimizing GWP.

The trade-off between costs and GWP was evaluated using a combined objective function. This analysis revealed that the marginal costs of an example day when prioritizing GWP over costs was ~0.4 DKK/kg-CO2-eq.

MPC performance was investigated over 51 days, showing how the control optimizing costs was 19.2%, 29.6% and 9.2% cheaper compared to controls optimizing for GWP, effluent N-concentrations, or the currently implemented rule based control strategy (RBC). Similarly, the control optimizing GWP resulted in 40.9%, 42.5%, 13.9% and 34.9% lower emissions than the other controls optimizing for costs, electricity consumption, effluent quality, and RBC respectively.

Comparison between objectives revealed a correlation between inter-diurnal difference in prices/GHG-emissions and the potential savings, where larger difference generally led to larger savings. This indicates that the current potentials might increase in a future energy objective with more fluctuating energy sources. Finally, it is concluded that as the different objectives led to contrasting dynamics and performance, it is important to actively consider the choice of objective.

Overall, this study demonstrates the flexibility of the chosen MPC framework, which can easily accommodate for additional terms in the objective functions, allowing WRRF operators to quickly adapt the plant operation to new management objectives and to face new performance requirements.

**Acknowledgements**

This work is partly funded by the Innovation Fund Denmark (IFD) under File No. 7038-00097B Peter A. Stentofts industrial PhD study; Stochastic Predictive Control of Wastewater Treatment Processes and File No. 7038-00097B.

**REFERENCES**

Ahn, J. H., Kim, S., Park, H., Rahm, B., Pagilla, K., & Chandran, K. (2010). N2O emissions from activated sludge processes, 2008-2009: Results of a national monitoring survey in the united states. Environmental Science and Technology, 44(12), 4505–4511. https://doi.org/10.1021/es903845y

733 Aymerich, I., Rieger, L., Sobhani, R., Rosso, D., & Corominas, L. (2015). The
734 difference between energy consumption and energy cost: Modelling energy tariff
735 structures for water resource recovery facilities. Water Research, 81, 113–123.
736 https://doi.org/10.1016/j.watres.2015.04.033

737 Bartram, D., Shart, M. D., Ebie, Y., Farkas, J., Gueguen, C., Peters, G. M.,
738 Zanzottera, N. M., Karthik, M., (2019), Chapter 6 – Wastewater treatment and
739 discharge, refinement to the 2006 IPCC guidelines for National Greenhouse Gas
740 Inventories, IPCC, Geneva, Switzerland

741 Bellandi, G., Weijers, S., Gori, R., & Nopens, I. (2020). Towards an online mitigation
742 strategy for N2O emissions through principal components analysis and clustering
743 techniques. Journal of Environmental Management, 261.
744 https://doi.org/10.1016/j.jenvman.2020.110219

745 Bernardelli, A., Marsili-Libelli, S., Manzini, A., Stancari, S., Tardini, G., Montanari,
746 D., Anceschi, G.. Gelli, P., Venier, S. (2020). Real-time model predictive control of a
747 wastewater treatment plant based on machine learning. Water Science and
748 Technology, 81(11), 2391–2400. https://doi.org/10.2166/wst.2020.298

749 Blum, J.-M., Jensen, M. M., & Smets, B. F. (2018a). Nitrous oxide production in
750 intermittently aerated Partial Nitritation-Anammox reactor: oxic N2O production
751 dominates and relates with ammonia removal rate. Chemical Engineering Journal
752 (1996. Print), 335, 458–466. https://doi.org/10.1016/j.cej.2017.10.146

753 Blum, J.-M., Su, Q., Ma, Y., Valverde Pérez, B., Domingo-Felez, C., Jensen, M. M.,
754 & Smets, B. F. (2018b). The pH dependency of N-converting enzymatic processes,

pathways and microbes: effect on net N2O production. Environmental Microbiology, 20(5), 1623–1640. https://doi.org/10.1111/1462-2920.14063

Brok, N.B., Stentoft, P.A., Munk-Nielsen, T., and Madsen, H. (2019). Flexible control of wastewater aeration for cost-efficient, sustainable treatment. IFAC-papersonline,52(4), 494–499. doi:10.1016/j.ifacol.2019.08.259.

Cao, S. Y., (2011) .Mass flow and energy efficiency of municipal wastewater treatment plants. IWA Publishing.

Carstensen, J., Harremoes, P., and Madsen, H. (1995). Statistical identification of monod-kinetic parametersfrom on-line measurements. Water Science and Technology, 31(2), 125–133.

Daelman, M. R. J., van Voorthuizen, E. M., van Dongen, U. G. J. M., Volcke, E. I. P., & van Loosdrecht, M. C. M. (2015). Seasonal and diurnal variability of N2O emissions from a full-scale municipal wastewater treatment plant. Science of the Total Environment, 536, 1–11. https://doi.org/10.1016/j.scitotenv.2015.06.122

Danish Ministry of Taxation (2020). Danish Wastewater Taxation Act. Bekendtgørelse af lov om afgift af spildevand (Spildevandsafgiftloven), LBK nr 478 af 14/04/2020. Danish Ministry of Taxation, Denmark.

Delre, A., ten Hoeve, M., & Scheutz, C. (2019). Site-specific carbon footprints of Scandinavian wastewater treatment plants, using the life cycle assessment approach. Journal of Cleaner Production, 211, 1001–1014. https://doi.org/10.1016/j.jclepro.2018.11.200

776 Domingo Félez, C., & Smets, B. F. (2016). A consilience model to describe $N_2O$
777 production during biological N removal. Environmental Science: Water Research and
778 Technology, 2(6), 923–930. https://doi.org/10.1039/C6EW00179C

779 Domingo-Félez, C., & Smets, B. F. (2019). Regulation of key N2O production
780 mechanisms during biological water treatment. Current Opinion in Biotechnology, 57,
781 119–126, 119–126. https://doi.org/10.1016/j.copbio.2019.03.006

782 Duan, Q., Y., Gupta, V., K., and Sorooshian, S. (1993). Shuffled complex evolution
783 approach for effective and efficient global minimization. Journal of Optimization
784 Theory and Applications, 76(3), 501–521.doi:10.1007/BF00939380.

785 Energinet. (2020). Energisystemet lige nu (English: ”Energisystem now”), Ballerup,
786 Denmark. https://energinet.dk/energisystem_fullscreen [visited 12-09-2020]

787 Escriva-Bou, A., Lund, J. R., & Pulido-Velazquez, M. (2018). Saving Energy From
788 Urban Water Demand Management. Water Resources Research, 54(7), 4265–4276.
789 https://doi.org/10.1029/2017WR021448

790 Foscoliano, C., Del Vigo, S., Mulas, M., & Tronci, S. (2016). Predictive control of an
791 activated sludge process for long term operation. Chemical Engineering Journal, 304,
792 1031–1044. https://doi.org/10.1016/j.cej.2016.07.018

793 Henze, M., Gujer, W., Mino, T., & van Loosdrecht, M. C. M. (2000). Activated
794 sludge models ASM1, ASM2, ASM2d and ASM3, Vol. 9, IWA Publishing.

795 Holenda, B., Domokos, E., Redey, A., & Fazakas, J. (2008). Dissolved oxygen
796 control of the activated sludge wastewater treatment process using model predictive

control. Computers and Chemical Engineering, 32(6), 1270–1278. https://doi.org/10.1016/j.compchemeng.2007.06.008

Isaacs, S., and Thornberg D. 1998. Rule Based Control of a Periodic Activated Sludge Process. Water Science and Technology 38 (3). doi:10.1016/S0273-1223(98)00468-5.Kirchem, D., Lynch, M., Bertsch, V., & Casey, E. (2018). Market effects of industrial demand response and flexibility potential from wastewater treatment facilities. International Conference on the European Energy Market, Eem, 2018-, 8469974. https://doi.org/10.1109/EEM.2018.8469974

Jeppsson, U., Pons, M. N., Nopens, I., Alex, J., Copp, J. B., Gernaey, K., … Vanrolleghem, P. A. (2007). Benchmark simulation model no 2: general protocol and exploratory case studies. Water Science and Technology, 56(8), 67–78. https://doi.org/10.2166/wst.2007.604

Kristensen K, Nielsen A, Berg CW, Skaug H, Bell BM (2016). "TMB: Automatic Differentiation and Laplace Approximation." Journal of Statistical Software, 70(5), 1–21. doi: 10.18637/jss.v070.i05.

Langergraber, G., Alex, J., Weissenbacher, N., Woerner, D., Ahnert, M., Frehmann, T., … Winkler, S. (2008). Generation of diurnal variation for influent data for dynamic simulation. Water Science and Technology, 57(9), 1483–1486. https://doi.org/10.2166/wst.2008.228

Leerbeck, K., Bacher, P., Junker, R. G., Goranović, G., Corradi, O., Ebrahimy, R., … Madsen, H. (2020a). Short-term forecasting of CO2 emission intensity in power grids by machine learning. Applied Energy, 277, 115527. https://doi.org/10.1016/j.apenergy.2020.115527

Leerbeck, K., Bacher, P., Junker, R. G., Tveit, A., Corradi, O., & Madsen, H. (2020b). Control of heat pumps with $CO_2$ emission intensity forecasts. Energies, 13(11), 2851. https://doi.org/10.3390/en13112851

Lindstrøm Sørensen, M., Dahl, P., Stentoft, P.A., Munk-Nielsen, T., and Kloppenborg Møller, J. (2019). Stochastic model predictive control of phosphorus concentration for smart power, cost-effective municipal wastewater treatment. Watermatex 2019, 10th IWA Symposium on Modelling and Integrated Assesment

Lisk, B., & Long, H. (2013). Demand management strategies resulting in "zero and low cost" energy saving opportunities for water and wastewater treatment facilities. 86th Annual Water Environment Federation Technical Exhibition and Conference, Weftec 2013, 3, 1705–1714. https://doi.org/10.2175/193864713813673316

Longo, S., d'Antoni, B. M., Bongards, M., Chaparro, A., Cronrath, A., Fatone, F., … Hospido, A. (2016). Monitoring and diagnosis of energy consumption in wastewater treatment plants. A state of the art and proposals for improvement. Applied Energy, 179, 1251–1268. https://doi.org/10.1016/j.apenergy.2016.07.043

Longo, S., Chitnis, M., Mauricio-Iglesias, M., and Hospido, A. (2020). Transient and persistent energy efficiency in the wastewater sector based on economic foundations. Energy Journal, 41(01). doi:10.5547/01956574.41.6.slon,10.5547/ISSN0195-6574-EJ

Lund, N. S. V., Falk, A. K. V., Borup, M., Madsen, H., & Mikkelsen, P. S. (2018). Model predictive control of urban drainage systems: A review and perspective towards smart real-time water management. Critical Reviews in Environmental

842 Science and Technology, 48(3), 279–339.
843 https://doi.org/10.1080/10643389.2018.1455484

844 Mulas, M., Tronci, S., Corona, F., Haimi, H., Lindell, P., Heinonen, M., … Baratti, R.
845 (2015). Predictive control of an activated sludge process: An application to the
846 Viikinmaki wastewater treatment plant. Journal of Process Control, 35, 89–100.
847 https://doi.org/10.1016/j.jprocont.2015.08.005

848 Nielsen, M. K., & Onnerth, T. B. (1995). Improvement of a recirculating plant by
849 introducing star control. Water Science and Technology, 31(2), 171–180.
850 https://doi.org/10.1016/0273-1223(95)00190-X

851 Nordpool, (2020), Market Data, Nordpool group, Oslo, Norway, Available at:
852 https://www.nordpoolgroup.com/Market-data1/#/nordic/table [visited 12-09-2020]

853 Olsson, G. (2015). "Water and Energy: Threats and Opportunities - Second Edition".
854 und. In:Water Intelligence Online14. ISSN: 14761777. DOI:10.2166/9781780406947

855 Porro, J., Bellandi, G., Rodriguez-Roda, I., Deeke, A., Weijers, S., Vanrolleghem, P.,
856 … Nopens, I. (2017). Developing an artificial intelligence-based WRRF nitrous oxide
857 mitigation road map: The Eindhoven N2O mitigation case study. Water Environment
858 Federation Technical Exhibition and Conference 2017, Weftec 2017, 3, 1568–1580.

859 REN21. 2020. Renewables 2020 Global Status Report, Paris: REN21 Secretariat,
860 ISBN 978-3-948393-00-7

861 Stentoft, P.A., Munk-Nielsen, T., Mikkelsen, P.S., and Madsen, H. (2017). A
862 stochastic method to manage delay and missing values for in-situ sensors in an alter-

nating activated sludge process. Proceedings of the 12th Iwa Specialized Conference on Instrumentation, Control and Automation.

Stentoft, P.A., Guericke, D., Munk-Nielsen, T., Mikkelsen,P.S., Madsen, H., Vezzaro, L., and Møller, J.K. (2019a).Model predictive control of stochastic wastewater treatment process for smart power, cost-effective aeration. Proceedings of Dycops 2019.

Stentoft, P.A., Munk-Nielsen, T., Vezzaro, L., Madsen,H., Mikkelsen, P.S., and Møller, J.K. (2019b). Towards model predictive control: online predictions of ammonium and nitrate removal by using a stochastic ASM. Water Science and Technology, 79(1), 51–62. doi:10.2166/wst.2018.527

Stentoft, P. A., Vezzaro, L., Mikkelsen, P. S., Grum, M., Munk-Nielsen, T., Tychsen, P., … Halvgaard, R. (2020a). Integrated model predictive control of water resource recovery facilities and sewer systems in a smart grid: example of full-scale implementation in Kolding. Water Science and Technology : a Journal of the International Association on Water Pollution Research, 81(8), 1766–1777. https://doi.org/10.2166/wst.2020.266

Tchobanoglous, G.; Burton, F.L; Stensel, H.D., 2004. Wastewater engineering treatment and reuse, 4th Edition. McGraw-Hill: New York.

Vasilaki, V., Volcke, E. I. P., Nandi, A. K., van Loosdrecht, M. C. M., & Katsou, E. (2018). Relating N2O emissions during biological nitrogen removal with operating conditions using multivariate statistical techniques. Water Research, 140, 387–402. https://doi.org/10.1016/j.watres.2018.04.052

885 Yamanaka, O., Obara, T., & Yamamoto, K. (2006). Total cost minimization control
886 scheme for biological wastewater treatment process and its evaluation based on the
887 COST benchmark process. Water Science and Technology, 53(4-5), 203–214.
888 https://doi.org/10.2166/wst.2006.125

889 Yuan, Z., Olsson, G., Cardell-Oliver, R., van Schagen, K., Marchi, A., Deletic, A.,
890 Urich, C., Rauch, W., Liu, Y., and Jiang, G. (2019). Sweating the assets the role of
891 instrumentation, control and automation in urban water systems. Water Research,
892 155, 381–402. doi:10.1016/j.watres.2019.02.034

893

## TABLES AND FIGURES

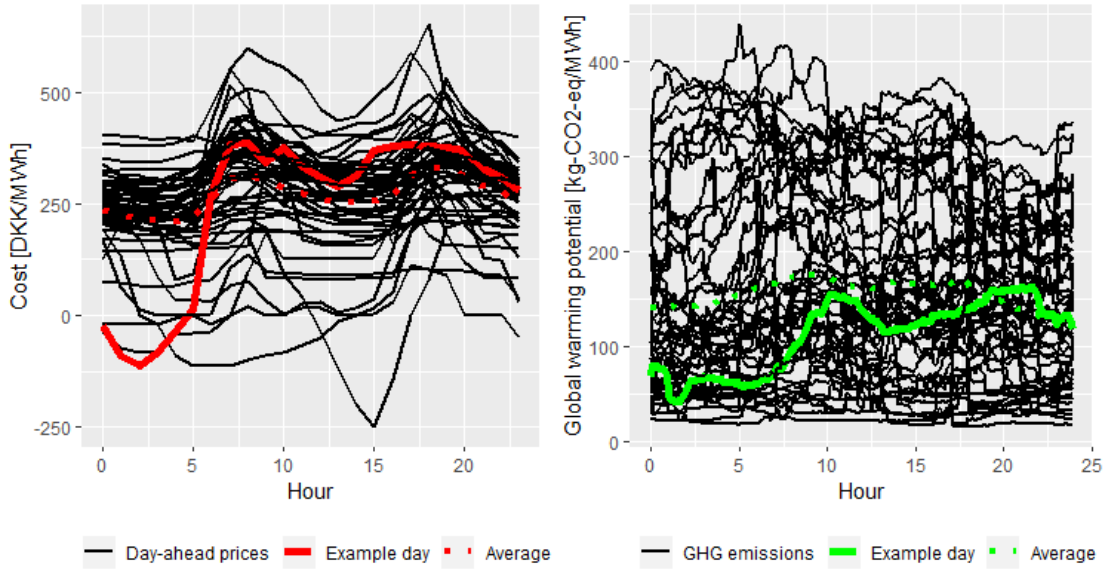


**Figure 1** Electricity prices for the Denmark West market (Nordpool, 2020) and (b) GHG emissions from electricity production (Energinet, 2020) for the Nordic electricity market, for the 51 days in the period from 2019/01/14 to 2020/02/18. The example day (2019/01/14) is highlighted.

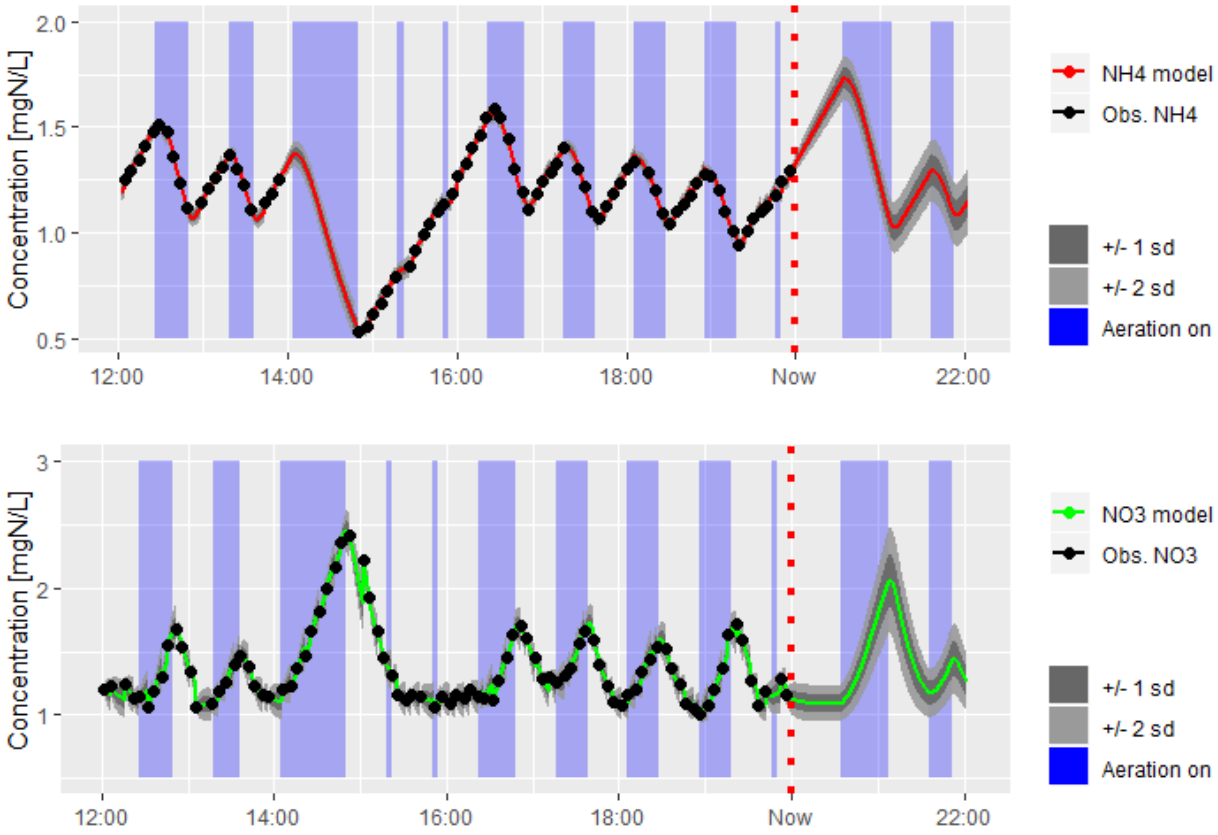


**Figure 2** Model fitted to ammonium and nitrate data from Nørre Snede WRRF for the example day (2019/01/14), including a prediction 2 hours ahead from 20:00 ("now"). The estimated parameters related to this fit are shown in Table 1. The grey areas highlight the uncertainty of the model predictions. Note that uncertainty increases as prediction horizon increases. This is to emphasize that the "known" observations are further back, and hence it is more difficult to predict accurately.

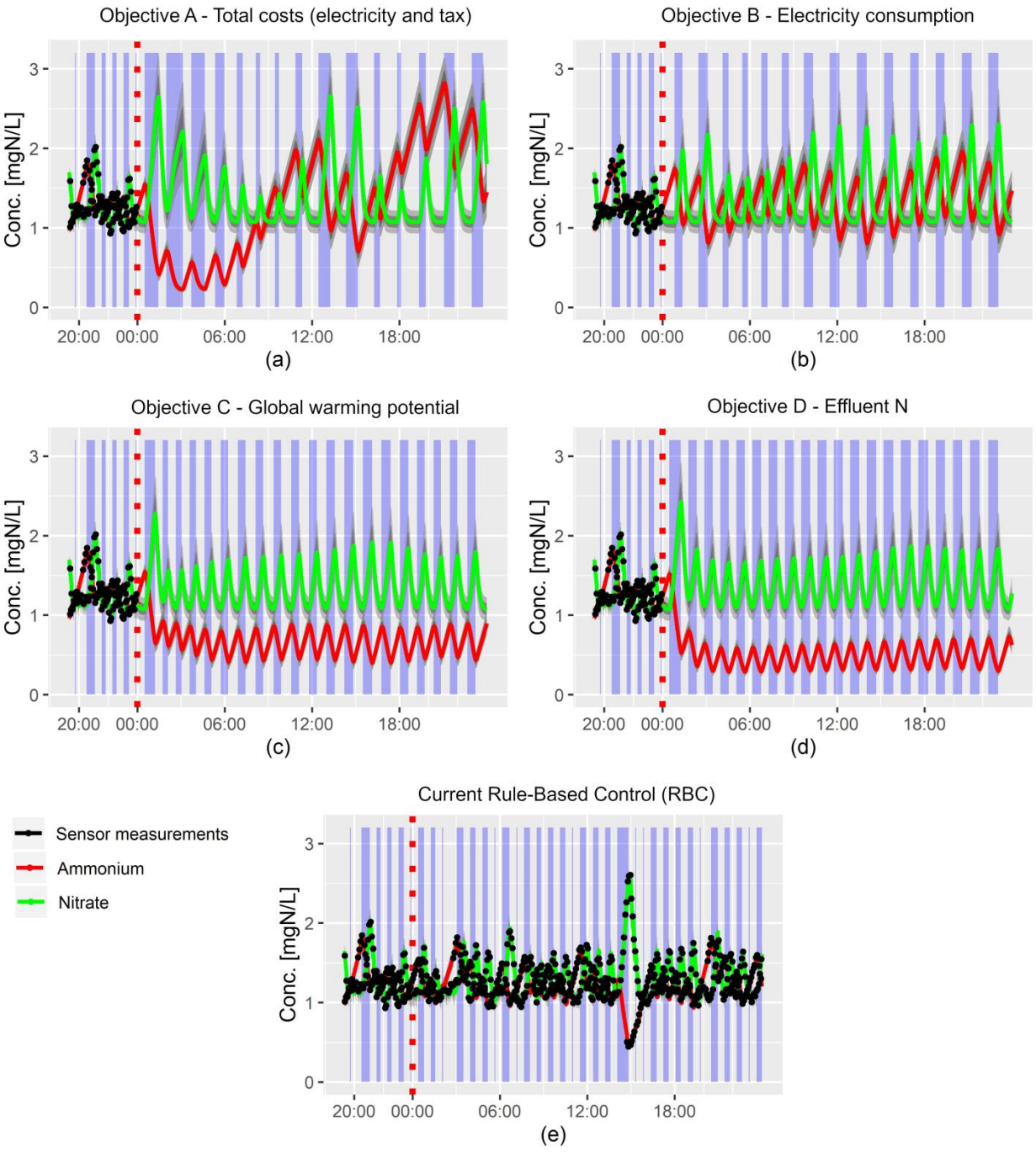


**Figure 3.** Ammonium and nitrate concentration and aeration controls obtained with different control scenarios 24 hours ahead (example day - starting from 2019/01/14 00:00): (a) optimization of total operational costs, (b) optimization of electricity consumption, (c), optimization of global warming potential, (d) optimization of effluent total-N, and (e) current rule-based control. Aeration phases are shown by the different background colors: on (blue) and off (grey).

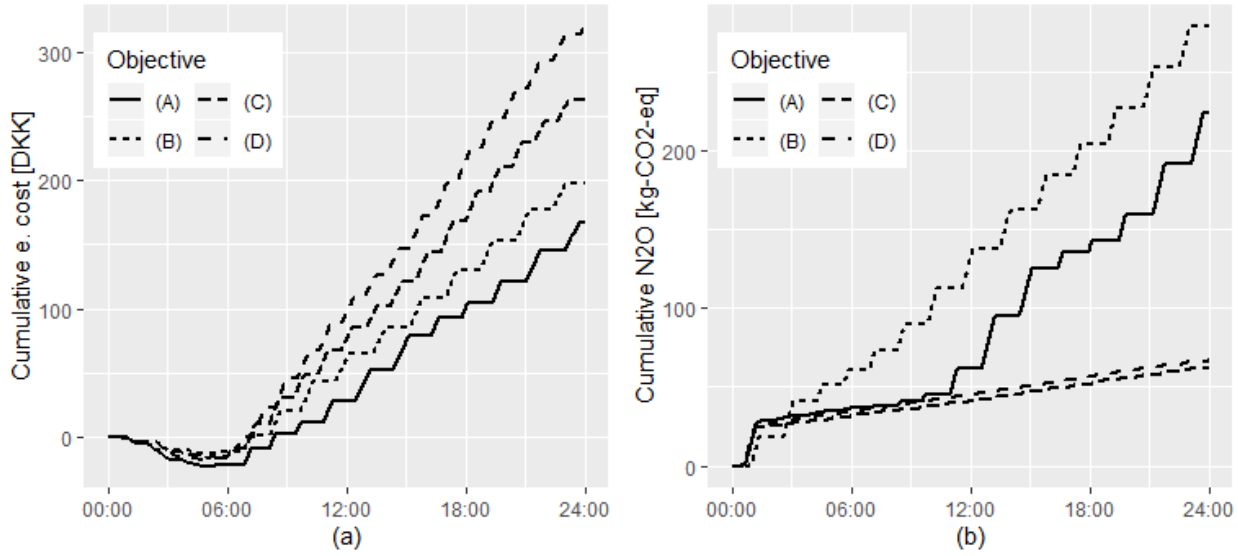


**Figure 4** (a) Cumulative electricity costs and (b) $N_2O$ emissions from process for the four control scenarios over the example day.

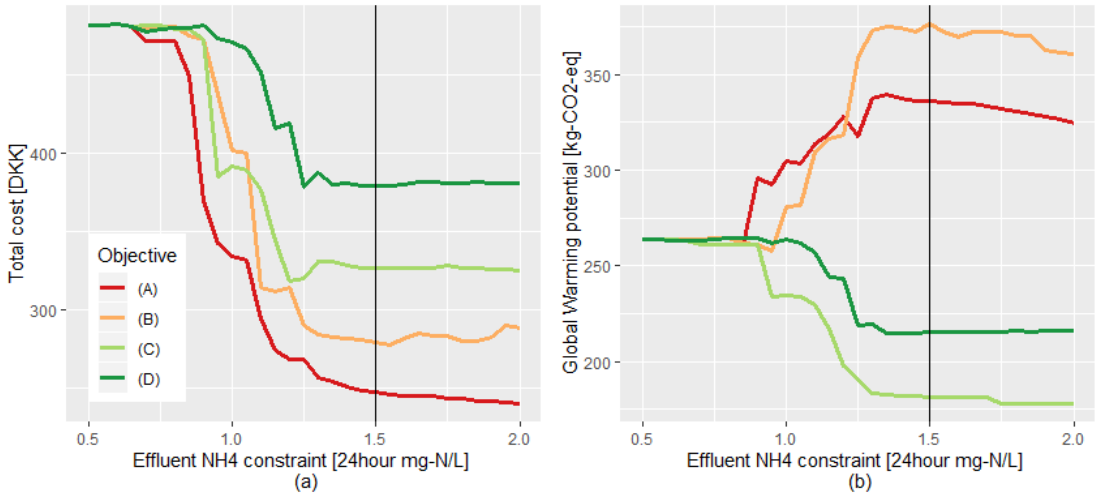


**Figure 5** Effect of different constraints on effluent NH4 concentration on (a) total costs and (b) GWP for different control scenarios on the example day. The black line shows the limit used for the results shown in Figure 2 and 3.

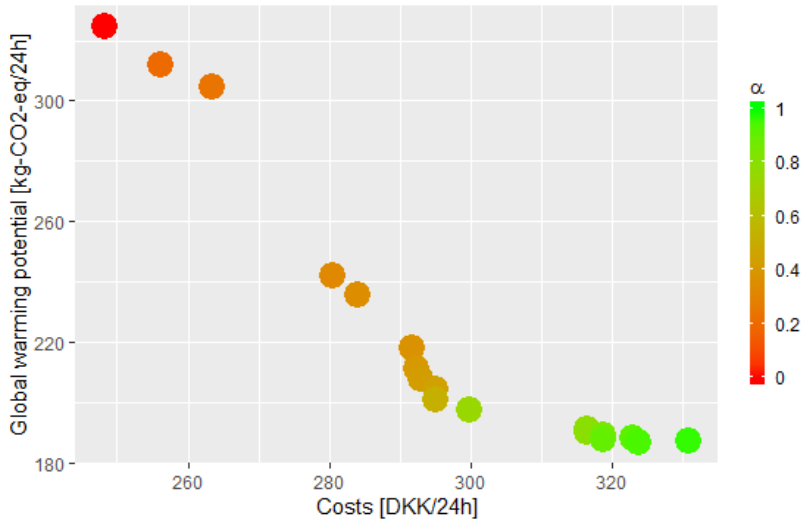


**Figure 6** Trade-off between total costs and global warming potential using a combined objective function (eq. 18) for the different values of $\alpha$ (α=0 corresponds to cost prioritization only, α=1 corresponds to GWP prioritization only).

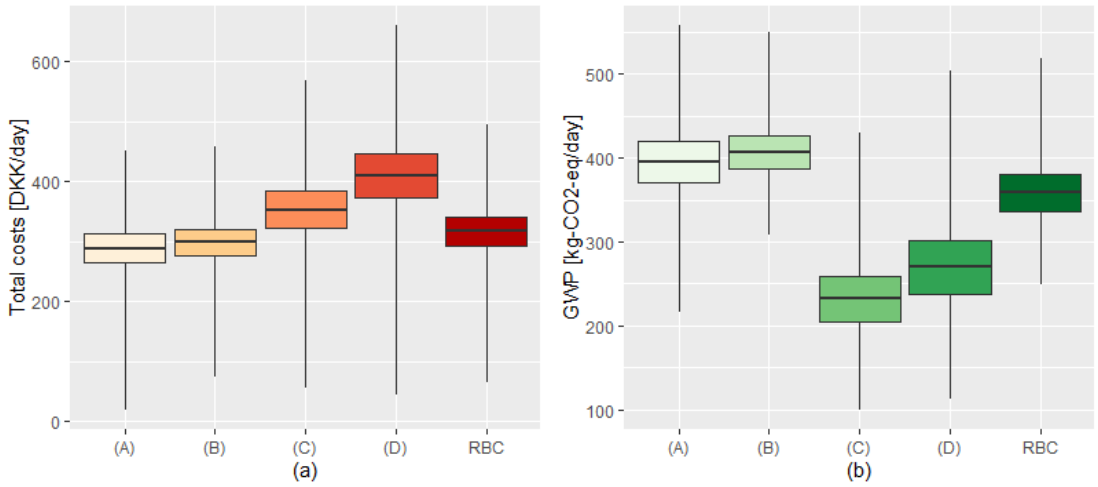


**Figure 7** Boxplots showing (a) total costs and (b) global warming potential obtained for the 51 simulated days (shown in Figure 1) by using the four control scenarios (A-D) and the current rule-based control (RBC). The boxplots show max/min (whiskers), +/- 2 standard deviations (coloured space) and the mean (horizontal black lines).

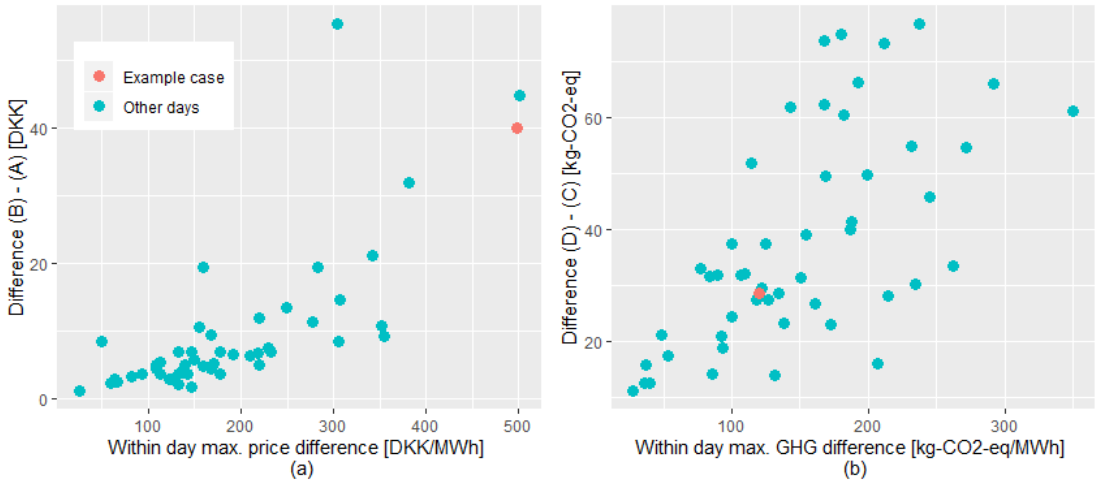


**Figure 8** (a) Difference in total daily cost between Objective A and B as a function of inter-diurnal price variations (max – min) (b) Difference in GWP between objectives C and D as a function of inter-diurnal variations in GHG emission from electricity production (min-max). Results are shown for the 51 simulated days, while the example day is marked in red.

**Table 1** List of parameters and state variables of the data-driven Activated Sludge Model for nitrogen removal. The last column shows the estimate obtained using 24 hours of ammonium and nitrate measurements from Nørre Snede WRRF on the example day (2019/01/14).

| *Parameter* | *Description* | *Unit* | *Estimate for example day* |
|---|---|---|---|
| $\kappa_1$ | Rate for incoming WW | [] | 0.27 |
| $\kappa_2$ | Rate for change in incoming $NH_4$ | [] | 0.62 |
| $r_{Ni}$ | Nitrification rate | $mgNL^{-1}min^{-1}$ | 0.05 |
| $r_{Dni}$ | Denitrification rate | $mgNL^{-1}min^{-1}$ | 0.11 |
| $m_{NH}$ | minimum observable $NH_4$ conc. | $mgNL^{-1}$ | 0.14 |
| $m_{NO}$ | minimum observable $NO_3$ conc. | $mgNL^{-1}$ | 0.92 |
| $K_{NH}$ | Monod inspired affinity coefficient for $NH_4$. | min | 1.81 |
| $K_{NO}$ | Monod inspired affinity coefficient for $NO_3$. | min | 1.97 |
| $\mu_{in,NH}$ | Mean incoming $NH_4$ conc. | $mgNL^{-1}$ | 67.9 |
| $\mu_{in,NO}$ | Mean incoming $NO_3$ conc. | $mgNL^{-1}$ | 0.01 (fixed) |
| $\sigma_1$ | Model noise parameter related to $S_{NH}$ | $mgNL^{-1}$ | 0.02 |
| $\sigma_2$ | Model noise parameter related to $S_{NO}$ | $mgNL^{-1}$ | 0.04 |
| $\sigma_3$ | Model noise parameter related to $S_\mu$ | $mgNL^{-1}$ | 0.06 |
| Aeration term, $O_j$ (eq. 5) | | | |
| $\kappa_3$ | Rate for skewness in the oxygen signal | [] | 3.00 |
| $\kappa_4$ | Rate for increase in oxygen after start | [] | 0.19 |
| $D_j$ | The "delay" of observations | min | 1.89 |
| $\tau_{on,i}$ | The switch aeration “on” times | min | Input |
| $\tau_{off,i}$ | The switch aeration “off” times | min | Input |
| State variables, $S_x$ | | | |
| $S_{NH}$ | Ammonium concentration in tank | $mgNL^{-1}$ | variable |
| $S_{NO}$ | Nitrate concentration in tank | $mgNL^{-1}$ | variable |
| $S_\mu$ | Inlet flux of incoming ammonium | $mgNL^{-1}$ | variable |

**Table 2** Parameter of the objective functions used in the optimization of the Nørre Snede WRRF.

| *Parameter* | *Description* | *Value* |
|---|---|---|
| $Ec$ | Equipment consumption [MW] | 0.1 |
| $T_N$ | Effluent tax [DKK/kg-N] | 30.0 |
| $L_{NH}$ | Ammonium limit [mg-N/L/24h] | 1.5 |
| $L_N$ | Total-N limit [mg-N/L/24h] | 2.9 |
| $\tau_{min,on}$ | Min duration of aeration phase [min] | 10 |
| $\tau_{max,on}$ | Max duration of aeration phase [min] | 80 |
| $\tau_{min,off}$ | Min duration of no-aeration phase [min] | 30 |
| $\tau_{max,off}$ | Max duration of no-aeration phase [min] | 80 |
| $C_{N_2O,CO_2}$ | $N_2O$ GWP-contribution [kg-CO2-eq/kg-N2O] | 298 |
| $Eff_{N_2O}$ | $N_2O$ produced due to effluent N | 0.005 |
| $r_{N_2O,low}$ | $N_2O$ emission $r_{NH}$<5mg TAN/(g-VSS*h) [] | 0.01 |
| $r_{N_2O,high}$ | $N_2O$ emission $r_{NH}$>5mg TAN/(g-VSS*h) [] | 0.09 |
| Z | Large number for the soft constraints | 10000 |
| VSS | Volatile suspended solids [g/L] | 3 |

**Table 3.** Performance indicators from application of the four different management objectives (A-D) and the current control (RBC) on the example day (Figure 1). The indicator targeting the goal of the objective functions is highlighted in bold and a frame. In addition the lowest value for each performance indicator is highlighted in bold. Effluent concentrations are estimated as average over 24 hours. Average electricity price/GWP are the obtained values over the 24 hours with variable inputs. $N_2O$ emissions cover both the direct and indirect $N_2O$.

| *Performance indicator* | *A* | *B* | *C* | *D* | *RBC** |
|---|---|---|---|---|---|
| Effluent NH4 [mgN/L] | 1.33 | 1.36 | 0.69 | **0.52** | 1.25 |
| Effluent NO3 [mgN/L] | 1.41 | 1.36 | 1.35 | 1.39 | **1.30** |
| Effluent total-N [mgN/L] | 2.74 | 2.72 | 2.04 | **1.91** | 2.55 |
| Total Cost [DKK] | **247.7** | 279.4 | 324.2 | 377.2 | 307.7 |
| Electricity cost [DKK] | **165.2** | 197.8 | 263.0 | 319.7 | 231.2 |
| Effluent tax [DKK] | 82.4 | 81.6 | 61.2 | **57.5** | 76.5 |
| Relative Aeration [% "on"-time] | 39.5 | **33.3** | 44.6 | 53.7 | 37.1 |
| Average price of consumed electricity [DKK/MWh] | **174.2** | 247.5 | 245.7 | 248.0 | 259.8 |
| Average GWP of consumed electricity [kg-CO2-eq/MWh] | **102.7** | 114.0 | 113.1 | 112.6 | 115.6 |
| GWP, $N_2O$ contribution[kg-CO2-eq] | 227.9 | 282.4 | **64.7** | 69.2 | 219.6 |
| GWP from electricity production [kg-CO2-eq] | 96.8 | **91.1** | 121.0 | 145.2 | 102.9 |
| GWP, total [kg-CO2-eq] | 324.6 | 373.5 | **185.7** | 214.4 | 322.5 |